ACS SENSORS

pubs.acs.org/acssensors Article

Dissolvable Polymer Valves for Sweat Chrono-Sampling in Wearable Paper-Based Analytical Devices

Andreu Vaquer, Enrique Barón,* and Roberto de la Rica*

Cite This: *ACS Sens.* 2022, 7, 488−494 Read Online

ACCESS | Metrics & More | Article Recommendations | Supporting Information

ABSTRACT: Paper sensors with colorimetric signal transduction mechanisms are promising for developing single-use wearable patches that only require a smartphone to quantify signals. However, measuring biomarker fluctuations with colorimetric wearable sensors requires implementing a chrono-sampling method for performing sequential measurements. In this article, we report on a chrono-sampling method that enables the fabrication of wearable devices made entirely of filter paper. It consists of using dried polymers as closed valves that deflect the flow of liquids to different transducers of a multisensor. As time passes by, the polymer dissolves and the valve opens. The sequential opening of the valves results in a succession of measurements that reveals fluctuations in the concentration of the target analyte. This concept was demonstrated with a paper multisensor capable of performing nine consecutive pH measurements. The device was also adapted for developing a urea biosensor that detects pH measurements generated by the hydrolysis of the analyte catalyzed by urease. The proposed analytical platform could monitor the pH of sweat with an accuracy and precision comparable to a laboratory-based method when worn during an exercise routine. The results shown here pave the way for developing colorimetric wearable biosensors that measure variations in the concentration of biomarkers such as glucose, lactate, creatinine, or uric acid over time.

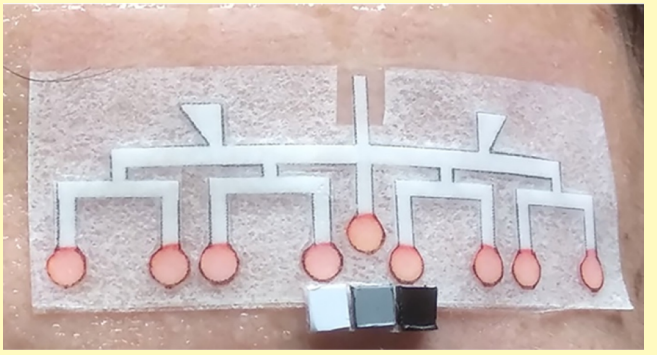

KEYWORDS: *colorimetric, microfluidic, smartphone, wearable, cellulose*

INTRODUCTION

Analytical devices that can be worn and provide continuous information about our health status are revolutionizing health care by enabling the effortless monitoring of biomarker fluctuations over time.[1−6] Among these, wearable devices that measure sweat biomarkers are becoming increasingly popular in sports medicine thanks to the noninvasive nature of the measurements.[7−10] Filter paper is an excellent candidate material to manufacture these platforms because it can absorb sweat and transport it to sensing areas through capillarity.[11−13] Furthermore, paper can be patterned using hydrophobic inks or papercutting, which makes it possible to design microfluidic platforms that transport liquids to a downstream outlet through wicking.[14−16] Paper is also bendable, which makes it suitable for developing sensing patches attached to the skin with medical adhesive.[12] Colorimetric signal generation mechanisms are the perfect match to these paper-based analytical devices because test outcomes can be recorded using the camera of a smartphone.[8,14] This type of readout is inherently wireless, which circumvents the need to implement antennae or any other type of circuity. This feature makes the resulting colorimetric sensors ideal as single-use devices that only require a disposable sticky patch and a smartphone to measure sweat biomarkers.

Implementing colorimetric signal generation mechanisms comes with challenges. In electrochemical wearable devices, sweat flows continuously over the transducer, which generates electrical signals that are related to the concentration of the analyte in real time. Colorimetric sensors often rely on the irreversible generation of color in a single spot.[8,12,14,17] Because of this, they require chrono-sampling to reveal fluctuations in biomarker levels over time.[18] This means that sweat samples are sequentially captured and measured independently with an array of colorimetric biosensors. In microfluidic devices made of polydimethylsiloxane (PDMS), this is accomplished by implementing capillary bursting valves that open at different pressures.[17] In paper-based analytical devices, valves that open via physical stimuli such as electroosmotic,[19] electrowetting,[20]

Received: October 22, 2021
Accepted: February 8, 2022
Published: February 16, 2022

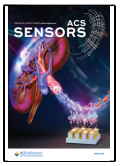

https://doi.org/10.1021/acssensors.1c02244
ACS Sens. 2022, 7, 488−494

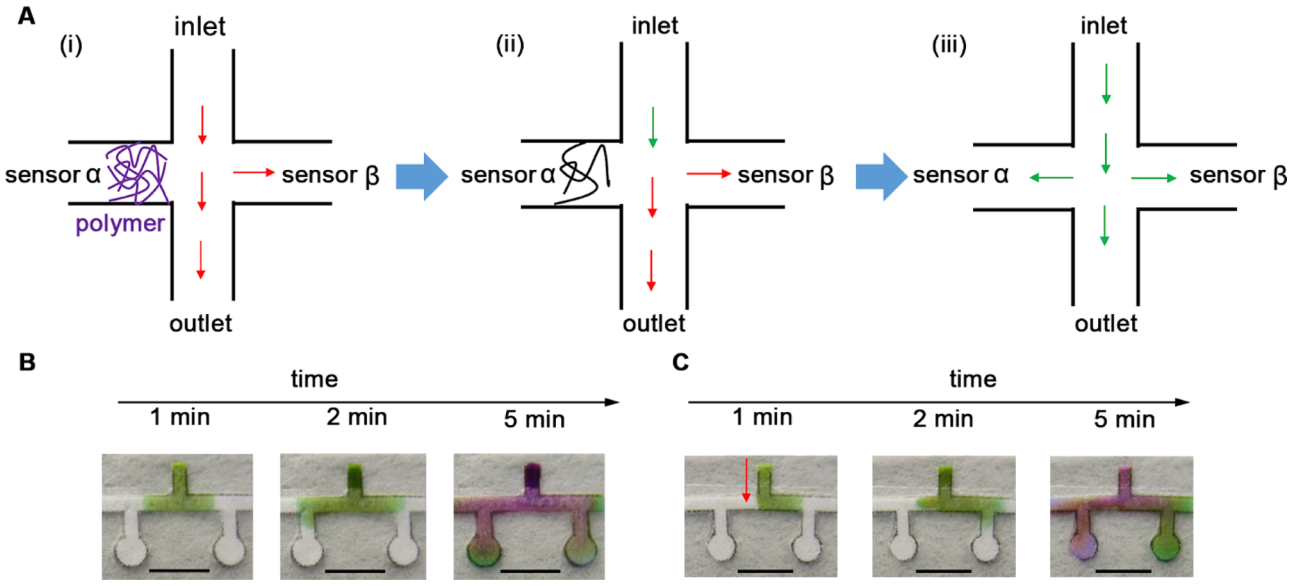

Figure 1. (A) Schematic representation and example of chrono-sampling with dissolvable polymer valves: (i) liquid of composition 1 (red arrows) enters the inlet and travels to sensor β and to the outlet because the path to sensor α is blocked by the polymer valve; (ii) as the polymer dissolves, the barrier thins out; and (iii) when the barrier dissolves, the valve opens and sweat of composition 2 (green arrows) can reach sensor α. As an example of chrono-sampling, green ink was added for 2 min before the addition of purple ink. (B) Without a dissolvable valve, the two inks arrive at the same time to the left and right destinations, where they mix. (C) Implementing a dissolvable barrier on the left channel (red arrow, two 0.5 μL drops of 7.5% PSS) drives the green ink preferentially to the right and, subsequently, the purple ink to the left. Scale bars, 0.5 cm.

magnetic,[21] mechanical,[22] or thermal[23,24] stimuli have been reported. However, implementing these valves in wearable sensors made of paper would require adding electrical actuators and circuitry to the design, which would increase the complexity of the fabrication process. Chemically actuated valves that open upon the addition of organic solvents[25] or surfactants[26] have also been reported. However, organic solvents need to be dispensed manually. An alternative to this is the implementation of dissolvable barriers made of sucrose, trehalose, or salts.[27,28] However, these are only meant to slow down liquid flow and therefore do not act as real valves that block fluids until they open up at a certain time. Because of this, they are better suited for timing the mixing of reagents than for enabling chrono-sampling schemes.[27,28] Alternatively, one could use polyvinyl alcohol (PVA), which has been shown to work as a dissolvable barrier in lateral flow tests, but it has never been used as a valve in chrono-sampling.[29] Other polymers such as pullulan have only been used to shut off liquid flow and are therefore not suitable for spacing out the release of reagents in wearable biosensors.[30]

In this article, we introduce a new approach for chrono-sampling in paper-based microfluidic devices. It is based on blocking fluid transport to different sensing areas with a coalesced water-soluble polymer such as polystyrene sulfonate (PSS) or polyvinyl alcohol (PVA) (Figure 1Ai). This ensures that sweat is collected in predetermined sensing elements. As the liquid flows, the polymer dissolves and the valve becomes thinner (Figure 1Aii). After a certain time defined by the flow rate and the polymer concentration, the valve completely dissolves and liquid flows to a new sensor (Figure 1Aiii). This approach ensures that the second sensor measures the composition of sweat that enters the inlet after a certain predetermined time and not the average composition of sweat since the beginning of the experiment. In Figure 1B,C, this concept is exemplified with the sequential addition of green and purple inks. Without valves, the sensing elements measure the same sample, which arrives to both sites at the same time (Figure 1B). Adding the dissolvable valve deflects the green ink to the right channel. Thanks to this, it is possible to first probe the composition of the green ink on the right sensor and to subsequently probe the composition of the purple ink on the left sensor, which is the principle behind chrono-sampling (Figure 1C). Increasing the number of valves and sensing elements increases the accuracy of sequential measurements because the time between measurements is reduced. Here, we show that combining this concept with a multichannel fluidic design allowed us to obtain nine measures over a period of ca. 20 min using colorimetric pH sensors as a proof of concept. The platform was worn as a sticky patch during an exercise routine, and pH measurements in sweat were comparable to those obtained with a laboratory-based method. These results pave the way for manufacturing wearable devices made entirely of paper that sequentially measure biomarker fluctuations over time without using external inputs to open and close valves.

EXPERIMENTAL SECTION

Reagents. Whatman filter paper Grade 41 (20 μm pore, cellulose, ashless), poly(sodium 4-styrenesulfonate) (PSS, 30% in water, average MW = 70,000), urease from jack beans (7.8 U/mg), urea, and poly(vinyl alcohol) (PVA, MW = 89,000−98,000) were purchased from Sigma-Aldrich. Purple, green, and blue water-based ink were purchased in a local mall. The pH-indicator solution (pH 4.0−10.0) was purchased from Merck Co. Medical tape adhesive was purchased from 3M.

Multisensor Fabrication. Designs were drawn with Adobe Photoshop, printed on Whatman paper, and subsequently cut by hand to produce microfluidic devices. pH sensors were obtained by adding four 1 μL drops of the universal pH indicator to the circular spots. Each drop was dried at room temperature before adding the next one. Using less than four drops reduced the sensitivity at high pH values (Figure S1). Soluble valves were obtained by adding 0.5 μL drops of PSS or PVA and drying them in an oven at 35 °C, which worked better than drying at room temperature (Figure S2). The drop-casting process was repeated to create valves with higher

https://doi.org/10.1021/acssensors.1c02244
ACS Sens. 2022, 7, 488−494

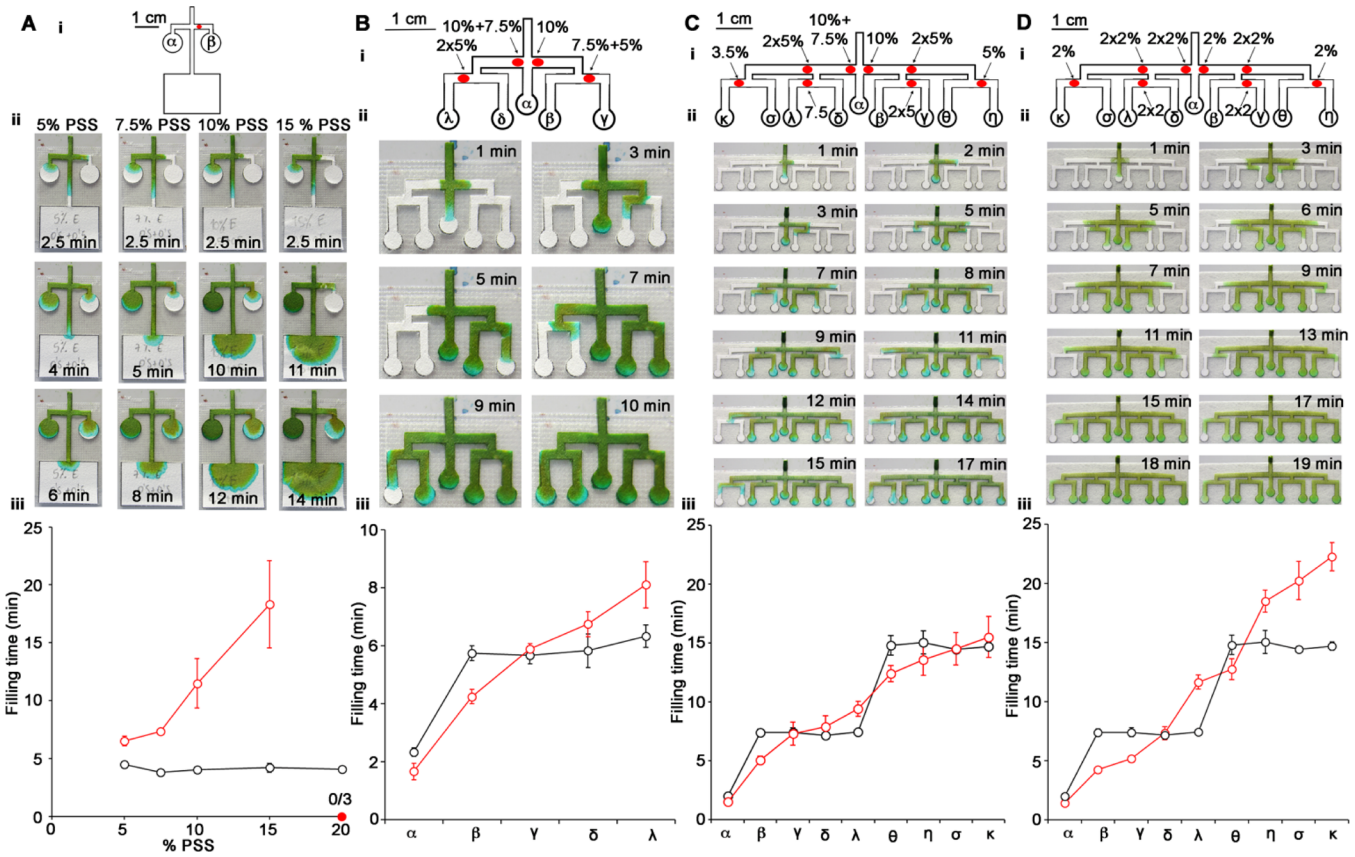

Figure 2. Microfluidic devices implementing dissolvable valves with increasing design complexity; valves in devices (A) to (C) were made with PSS, whereas valves in (D) were made with PVA. (i) Designs showing the regions where valves were implemented (red spots) and how they were fabricated (number of drops and % PSS in them); (ii) images showing liquid flow with time (from top to bottom); (iii) (a) time required to fill area α (black) or β (red) as a function of the % PSS; (b–d), time required to fill different areas α to κ shown in (i) with (red) or without (black) polymer valves. Error bars are the standard deviation of three different microfluidic platforms. The red spot on the x axis in (Aiii) indicates that the valve opened zero out of three times when fabricated with 20% PSS.

polymer content as explained in the text. The total amount of polymer in each valve was optimized by adding one or several drops of PSS at different % (v/v) in order to achieve a sequence of measurements spaced over time (Figures S3 to S5). Wearable biosensors were obtained by sandwiching the platform with medical adhesive to avoid contact with the skin everywhere except for the inlet. A three-color chart was added to equalize the color. This reduces artifacts in color quantification originating from varying photographic conditions.[14]

Characterization of the Microfluidic System. The sequential opening of valves was studied by adding water-based ink at a rate of 4 μL min^{-1} (1 μL every 15 s). The filling time was calculated as the time required to fill up the circular area of each sensing element in the design since the onset of the experiment.

pH Measurements. Calibration solutions were made from artificial sweat, prepared as described elsewhere[31] and adjusted to the desired pH with HCl. A standard tabletop pH meter was used to measure the pH of the solutions. A calibration curve was obtained by adding solutions of known pH through the inlet and measuring the colorimetric signal of the reservoirs. The calibration was carried out at room temperature for experiments aimed at demonstrating the performance of the multisensor and at 37 °C to evaluate pH changes when the device is worn during an exercise routine (Figure S6). The colorimetric signal was taken as the ratio between the pixel intensity in the G channel over the pixel intensity of the RGB channel (Green/RGB; Figure S7).

Urea Biosensor. The pH multisensor was transformed into a urea biosensor by adding 0.7 μL of 0.5 mg mL^{-1} urease in each sensor of the device. Calibration plots were obtained by adding urea at different concentrations. The colorimetric signal was taken as the pixel intensity of the RGB channel because it yielded the best results in the proposed concentration/color range.

pH Measurements as Wearable Sensors. The multisensor was fixed on the skin of volunteers with medical tape. The volunteers were asked to ride a static bicycle for at least 20 min to stimulate the production of sweat. The area was then cleaned, and the sensor was affixed. Sweat samples were also collected in Eppendorf tubes to compare the performance of the wearable devices with the laboratory-based method (Figure S8). The method consisted of mixing 20 μL of sweat with 50 μL of commercial pH indicator) in a 96-well plate followed by measuring the absorbances at 420 and 620 nm. The colorimetric signal was obtained by calculating the ratio between both measures (Abs_{420}/Abs_{620}). The protocol of these experiments was approved by the Balearic Islands Ethics Committee (IB 4053/19 PI). Informed consent was obtained from the participants.

RESULTS AND DISCUSSION

Microfluidics with Polymer Valves. Figure 2Ai shows our first prototype consisting in two channels arriving to round areas, an inlet and a squared outlet. The round areas α and β are meant to contain sensing elements or ramifications in future developments. The right channel is blocked with a valve made of PSS using different initial concentrations. The time-dependent liquid flow of green ink is shown from top to bottom (Figure 2Aii). In the absence of PSS, both channels fill up at the same time. The valve made of 5% PSS blocks the entry of ink to the right channel for 2.5 min. Consequently, the liquid is deflected to the left channel α, which fills up faster

https://doi.org/10.1021/acssensors.1c02244
ACS Sens. 2022, 7, 488–494

than β. The ability of deflecting liquids makes the proposed polymer better suited for fabricating valves than previous dissolvable materials, which could only slow down liquid flow.[27,28] In Figure 2Aiii, the time required to fill β increases as the % PSS increases. For example, when the concentration of PSS is 15%, it takes ca. 18 min to fill β, whereas it only takes 6 min when using 5% PSS. In fact, with an even higher % of PSS (20%) the valve never opens in the proposed experimental conditions. As the % PSS increases, it is also difficult to control the valve opening time with precision, as shown by the higher error bars in filling time measures in Figure 2Aiii. This issue can be ameliorated by drying the polymer in an oven at 37 °C instead of letting it dry at room temperature (Figure S10). Nevertheless, Figure 2Aiii shows that there is a linear relationship between the % PSS and the filling time calculated from three different microfluidic platforms. All in all, these experiments demonstrate that it is possible to block fluid flow with polymer valves and time their opening by changing the concentration of polymer in them. PSS concentrations between 5 and 10% yield valves with reproducible opening times. Below, we explore several multichannel devices that were designed following these principles.

The next step was to increase the complexity of the design to include different ramifications and valves. Figure 2Bi shows a second-generation device capable of performing five sequential measurements. Valves that opened at different times were obtained by spotting polymer solutions at different concentrations one or several times and drying them at 37 °C (Figure S10). This is indicated in the scheme on top of the figure. In this design, as the liquid enters through the inlet the left and right valves block liquid flow, which is directed to area α. The right valve is made with a single drop of 10% PSS, whereas the left valve is made with drops containing 10 and 7.5% PSS, respectively. The right valve opens first because it contains less PSS and liquid arrives to area β (Figure 2Bii). After a couple of minutes, the valve blocking the path to γ opens up and the liquid entering the outlet arrives to this area. The left channel follows a similar design, which was programmed to allow liquids to reach δ first and λ afterward. Figure 2Biii shows that the different areas α to λ fill up sequentially at a fixed time interval of 2 ± 0.75 min (red trace; see also Figure S3). In devices without polymer valves, the fluid arrives at the same time to areas β, γ, δ, and λ in the microfluidic devices (black trace), which means that they are not suitable for chrono-sampling. We then manufactured and tested a third generation of microfluidic devices capable of performing nine sequential measurements. Valves were made of PSS or PVA (Figure 2C,D). PSS valves open sequentially at 1.9 ± 1.0 min intervals during ca. 15 min, whereas PVA valves open at 2.5 ± 1.6 min intervals during a total time of 22 min. This means that sequential pH changes happening within 2 min may not be detected properly because chrono-sampling with our devices is not precise enough to separate them. Designs without valves had areas β to λ and θ to κ filled at the same time, and therefore, they were not suitable for chrono-sampling (black dots in Figure 2Ciii,Diii). These experiments demonstrate that it is possible to space out the arrival of liquid to different areas of paper-based microfluidic devices using polymer valves. In this approach, the valve opening time can be fine-tuned by changing the concentration and the type of polymer used to manufacture it. Supporting experiments show that the valves also change the flow speed through the microfluidic device, either because the polymer increases the viscosity or because valve opening splits the liquid into different channels (Figure S11 and Table S1).

pH Multisensor. We then sought to develop an analytical platform for monitoring the pH of sweat using the design shown in Figure 2D. Circular areas were modified with a pH indicator, and the sensors were calibrated with solutions adjusted at different pH values. Different pH values generate different colors in the spots that were quantified as the ratio between the green and RGB channels in the pH range between 5 and 7.5 (Figure S7). It was observed that dissolved PSS valves notoriously changed the pH of the sample being analyzed (Figure S9A,B). PVA valves had a negligible impact on the pH, and therefore, they were chosen to develop the device (Figure S9C). Figure 3A shows the sequential measurements when the multisensor was tested with a solution buffered at pH 7. Different sensing areas α to κ register an increase in the colorimetric signal as the valves blocking the path to reach them open. Using this design, the multisensor was able to sequentially measure the pH during 20 min when adding the buffer at a rate of ca. 4 μL min^{-1}. Figure 3B shows the calibration plot obtained at different pH values, which demonstrates that the proposed analytical platform can detect variations in pH within the physiological range.[32] The error bars are the standard deviation of the nine measurements performed within the platform. Therefore, they show the intrasensor variability, which was lower than 0.02 for all the pH values assayed.

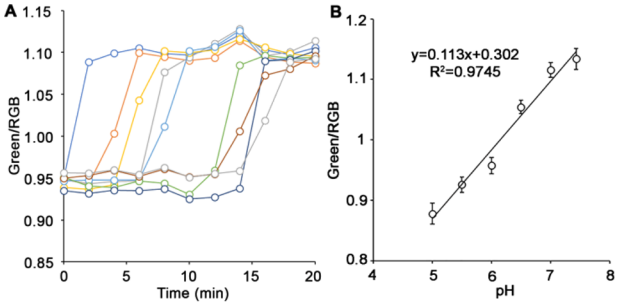

Figure 3. Detection of pH with the design shown in Figure 2D. (A) Colorimetric signal registered at different sensors in the platform over time (α, blue; β, orange; γ, yellow; δ, light gray; λ, light blue; θ, green; η, brown; σ, dark blue; κ, gray). (B) Calibration plot obtained by testing the full platform with solutions at a fixed pH value. Error bars are the standard deviation of the nine sensors within the platform.

Sequential pH Measurements. After demonstrating that the sensors in the analytical platform can detect pH variations reproducibly, we sought to determine whether the wearable device could monitor changes in the pH of the sample over time. To this end, we challenged the multisensor with a sequence of solutions adjusted at pH 7.22, 5.5, and 7.22, as well as with a sequence of solutions adjusted at pH 5.5, 7.22, and 5.5. In Figure 4A, the multisensors register the first pH variation with acceptable precision and accuracy, yielding a peak value of 5.63 ± 0.11 and 6.9 ± 0.21, respectively. However, the second pH step cannot be measured accurately, yielding peak values of 6.59 ± 0.11 and 6.39 ± 0.1. These readings substantially differ from the values in the calibrating solutions (7.22 and 5.5, respectively). This happened because there is a large dead volume where both solutions can mix, which changes their pH before arriving to the sensors in the platform. Increasing the number of sensors in the device could

https://doi.org/10.1021/acssensors.1c02244
ACS Sens. 2022, 7, 488−494

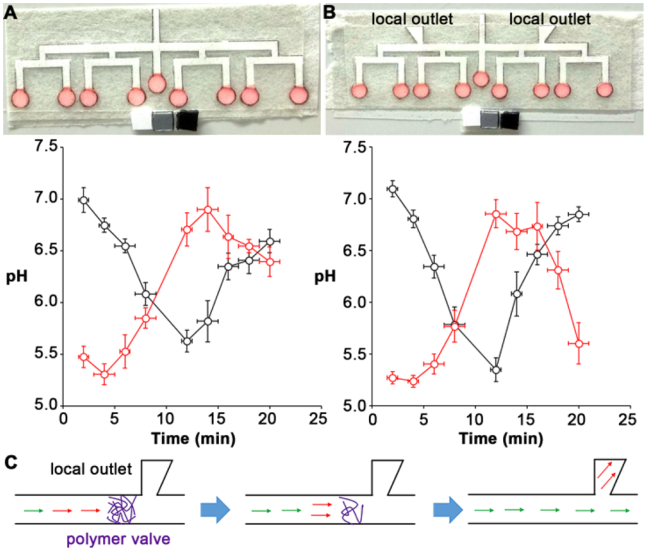

Figure 4. Detection of sequential changes in pH (from 5.5 to 7.22 to 5.5 (red) or from 7.22 to 5.5 to 7.22 (black) through chrono-sampling). (A) Design without local outlets. (B) Design implementing local outlets. (C) Scheme showing how local outlets work. Error bars are the standard deviation of three different analytical platforms.

solve this issue because more measurements would be performed. Valves could be redesigned so that they open later, which would also increase the total assay time. Here, we explore another way to increase the measurement time by adding local outlets at strategic positions of the design. The outlets are meant to help evacuate the solution before it arrives to the sensors, thus reducing the amount of mixed sample arriving to the sensing area and increasing the measurement time (Figure 4C). In Figure 4B, after implementing the local outlets, measurements of the second pH change can be registered with higher accuracy, yielding values of 5.6 ± 0.2 and 6.85 ± 0.07, respectively. Adding more sensing elements in the design could further improve the accuracy by reducing the time between successive measurements, which is essential to register time-resolved variations in the composition of the sample. Furthermore, adding an adjacent sweat volume sensor would help compensate for different sweat rates in real applications.[12,14] These experiments validate the proposed analytical platform for monitoring variations in pH over time through chrono-sampling.

Urea Biosensor. Next, we explored the idea of transforming our pH multisensor into a biosensor for urea monitoring. To this end, we added urease in the pH sensing elements. Urease catalyzes the hydrolysis of urea into ammonia and carbon dioxide, which increases the pH of the solution.[33] Figure 5A shows the colorimetric signal obtained after adding urea at different concentrations. The biosensors show a linear response in the concentration range between 5 and 30 mM, which fits well with physiological levels of this biomarker in sweat.[2] Figure 5B shows the results obtained by individual biosensors within the platform when these were queried with a solution of either 5 or 30 mM urea. All the biosensors performed similarly, with an intrasensor variability within the multisensor of 1.5 and 1.9% upon addition of 5 and 30 mM urea, respectively. Finally, we examined whether the multisensor could detect a change in the concentration of urea from 30 to 5 mM or vice versa through chrono-sampling. In Figure 5C, it is possible to follow the increase or decrease in concentration thanks to the sequential measurements performed by the multisensor. These experiments demonstrate that the proposed microfluidic platform is suitable for developing wearable biosensors that measure sequential changes in biomarker levels through chrono-sampling.

Sweat Measurements. Finally, we explored the adequacy of the proposed analytical platform for measuring sweat pH when worn during an exercise routine. Figure 6 shows the proposed analytical platform worn by a volunteer. The multisensor is placed directly onto the skin with medical

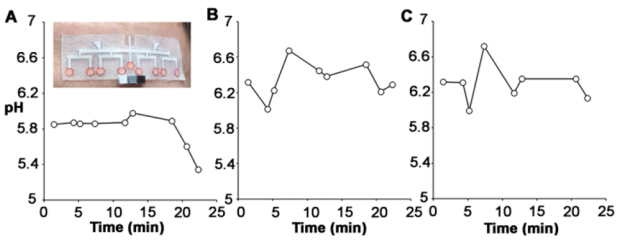

Figure 6. pH measurements performed with the sensor worn during an exercise routine: (A) volunteer 1; (B) and (C) volunteer 2. Inset shows a photograph of the sensing patch.

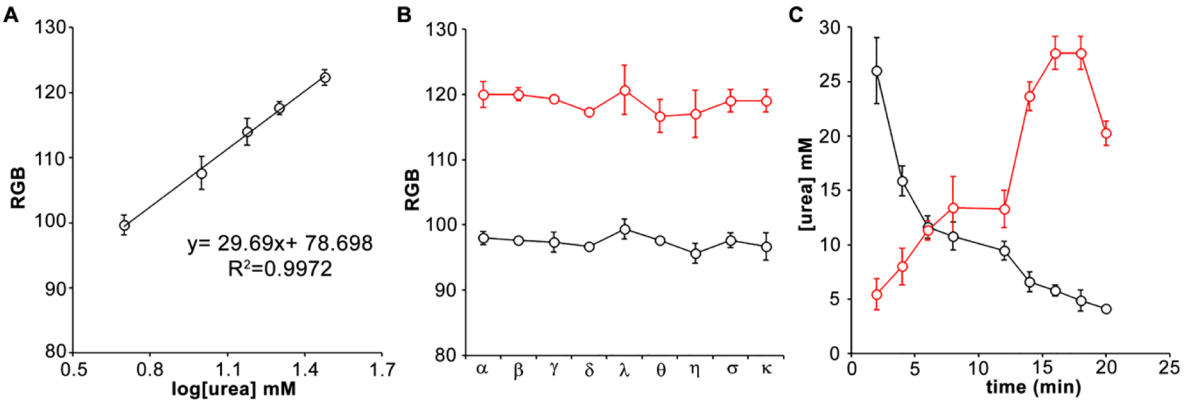

Figure 5. Urea multisensor based on detecting pH changes generated by urease. (A) Calibration plot showing the variation of the pixel intensity in the RGB channel with the logarithm of the concentration of urea. (B) Colorimetric signal generated in each of the sensors after adding 5 (black) or 30 (red) mM urea. (C) pH variations measured through chrono-sampling after adding 5 mM urea for 4 min followed by 30 mM urea (red) or 30 mM urea for 4 min followed by 5 mM urea (black). Error bars are the standard deviation of three independent multisensors.

https://doi.org/10.1021/acssensors.1c02244
ACS Sens. 2022, 7, 488−494

adhesive, where it wicks sweat through the inlet. The volunteers were asked to ride a static bicycle in order to produce sweat and demonstrate the possibility of sequentially measuring its pH with the proposed analytical platform. Sweat samples were collected during the first 9−10 min in tubes and analyzed with a laboratory-based method. Figure 6A shows the pH measurements obtained from the first volunteer. The wearable sensor registered a pH decrease from 5.85 to 5.35, whereas with the reference method, the pH values followed the same trend but were slightly higher (from 6.3 to 5.8). Figure 6B,C shows the results of two analytical platforms worn simultaneously by another volunteer. The pH values did not show any trend. Instead, they oscillated between 6 and 6.7 (average 6.3 ± 0.2) and between 6.1 and 6.7 (average 6.3 ± 0.2), respectively. This indicates that different sensors yield similar results when tested under similar conditions. The laboratory method yielded values between 6.5 and 6.7 (average 6.5 ± 0.1). This means that in all studied cases, the reference method yields pH values that are, on average, 0.2 units higher than the paper-based analytical platform. This indicates a potential source of bias, which nevertheless is not statistically significant (t test, $p > 0.05$).

CONCLUSIONS

In conclusion, we have introduced a method for sampling and analyzing sweat in a sequential manner with wearable paper-based devices. It features temporarily blocking fluid flow with dissolvable polymer valves. The time required to open the valve can be fine-tuned by controlling the amount of polymer deposited, for example, by adding drops of different polymer concentration in the region of interest and letting them dry. The concept of this design was proven with a multisensor capable of registering changes in the pH of a test solution over time. The design was adapted for developing a urea biosensor that detects pH measurements generated by the hydrolysis of urea catalyzed by urease. Results obtained when measuring changes in the pH of sweat when the sensor was worn by volunteers were comparable to those obtained with a laboratory-based method. Multiplying the endpoints α to κ by subdividing the connecting channel into multiple branches leading to different sensing elements could enable measuring several biomarkers at the same time. Future designs will focus on implementing different biosensors in the platform as well as changing the dimensions and number of local outlets in the microfluidic design in order to fine-tune the time elapsed between measurements.

ASSOCIATED CONTENT

Supporting Information

The Supporting Information is available free of charge at https://pubs.acs.org/doi/10.1021/acssensors.1c02244.

(Figure S1) Optimization of the amount of pH indicator in the sensing elements; (Figure S2) impact of drying temperature on valve fabrication; (Figure S3) optimization of chrono-sampling with a device implementing five sensing elements; (Figure S4) optimization of chrono-sampling with a device implementing nine sensing elements; (Figure S5) mass of dried polymer as a function of the volume and concentration; (Figure S6) calibration plot at 37 °C; (Figure S7) colorimetric signal as a function of the parameter selected for quantifying the pixel intensity with Adobe Photoshop; (Figure S8) laboratory-based method calibration curve; (Figure S9) impact of PSS and PVA in pH measurements; (Figure S10) impact of drying temperature in valve opening; (Figure S11) impact of polymer concentration on flow speed; (Table S1) flow speed measured in different channels of the microfluidic design (PDF)

AUTHOR INFORMATION

Corresponding Authors

Enrique Barón − *Multidisciplinary Sepsis Group, Health Research Institute of the Balearic Islands (IdISBa), Son Espases University Hospital, 07120 Palma de Mallorca, Spain;* orcid.org/0000-0001-7461-4599; Email: enrique.baron@ssib.es

Roberto de la Rica − *Multidisciplinary Sepsis Group, Health Research Institute of the Balearic Islands (IdISBa), Son Espases University Hospital, 07120 Palma de Mallorca, Spain; Department of Chemistry, University of the Balearic Islands, 07122 Palma de Mallorca, Spain;* orcid.org/0000-0002-5750-1469; Email: roberto.delarica@ssib.es

Author

Andreu Vaquer − *Multidisciplinary Sepsis Group, Health Research Institute of the Balearic Islands (IdISBa), Son Espases University Hospital, 07120 Palma de Mallorca, Spain; Department of Chemistry, University of the Balearic Islands, 07122 Palma de Mallorca, Spain*

Complete contact information is available at: https://pubs.acs.org/10.1021/acssensors.1c02244

Author Contributions

The manuscript was written through contributions of all authors. All authors have given approval to the final version of the manuscript.

Notes

The authors declare no competing financial interest.

ACKNOWLEDGMENTS

R.d.l.R. acknowledges funding from IdISBa/Impost turisme sostenible/Agència d'Estratègia Turística de les Illes Balears-Govern de les Illes Balears through a Radix fellowship. E.B. acknowledges funding from the Instituto de Salud Carlos III (Sara Borrell contract). A.V. acknowledges funding from the European Social Fund (ESF) through the JoTReSdOS program and a predoctoral fellowship FI/00167 from Instituto de Salud Carlos III co-financed from European Social Fund (FSE+) and Instituto de Salud Carlos III.

REFERENCES

(1) Ortega, L.; Llorella, A.; Esquivel, J. P.; Sabaté, N. Paper-Based Batteries as Conductivity Sensors for Single-Use Applications. *ACS Sens.* **2020**, *5*, 1743−1749.

(2) Hussain, S.; Park, S. Sweat-Based Noninvasive Skin-Patchable Urea Biosensors with Photonic Interpenetrating Polymer Network Films Integrated into PDMS Chips. *ACS Sens.* **2020**, *5*, 3988−3998.

(3) Choi, D.-H.; Gonzales, M.; Kitchen, G. B.; Phan, D.-T.; Searson, P. C. A Capacitive Sweat Rate Sensor for Continuous and Real-Time Monitoring of Sweat Loss. *ACS Sens.* **2020**, *5*, 3821−3826.

(4) Hozumi, S.; Honda, S.; Arie, T.; Akita, S.; Takei, K. Multimodal Wearable Sensor Sheet for Health-Related Chemical and Physical Monitoring. *ACS Sens.* **2021**, *6*, 1918−1924.

(5) Xu, S.; Fan, Z.; Yang, S.; Zuo, X.; Guo, Y.; Chen, H.; Pan, L. Highly Flexible, Stretchable, and Self-Powered Strain-Temperature

Dual Sensor Based on Free-Standing PEDOT:PSS/Carbon Nanocoils−Poly(Vinyl) Alcohol Films. *ACS Sens.* **2021**, *6*, 1120−1128.
(6) He, X.; Yang, S.; Pei, Q.; Song, Y.; Liu, C.; Xu, T.; Zhang, X. Integrated Smart Janus Textile Bands for Self-Pumping Sweat Sampling and Analysis. *ACS Sens.* **2020**, *5*, 1548−1554.
(7) Vinoth, R.; Nakagawa, T.; Mathiyarasu, J.; Mohan, A. M. V. Fully Printed Wearable Microfluidic Devices for High-Throughput Sweat Sampling and Multiplexed Electrochemical Analysis. *ACS Sens.* **2021**, *6*, 1174−1186.
(8) Zhang, K.; Zhang, J.; Wang, F.; Kong, D. Stretchable and Superwettable Colorimetric Sensing Patch for Epidermal Collection and Analysis of Sweat. *ACS Sens.* **2021**, *6*, 2261−2269.
(9) Xuan, X.; Pérez-Ràfols, C.; Chen, C.; Cuartero, M.; Crespo, G. A. Lactate Biosensing for Reliable On-Body Sweat Analysis. *ACS Sens.* **2021**, *6*, 2763−2771.
(10) Ghaffari, R.; Yang, D. S.; Kim, J.; Mansour, A.; Wright, J. A., Jr.; Model, J. B.; Wright, D. E.; Rogers, J. A.; Ray, T. R. State of Sweat: Emerging Wearable Systems for Real-Time, Noninvasive Sweat Sensing and Analytics. *ACS Sens.* **2021**, *6*, 2787−2801.
(11) Saha, T.; Fang, J.; Mukherjee, S.; Dickey, M. D.; Velev, O. D. Wearable Osmotic-Capillary Patch for Prolonged Sweat Harvesting and Sensing. *ACS Appl. Mater. Interfaces* **2021**, *13*, 8071−8081.
(12) Vaquer, A.; Barón, E.; de la Rica, R. Wearable Analytical Platform with Enzyme-Modulated Dynamic Range for the Simultaneous Colorimetric Detection of Sweat Volume and Sweat Biomarkers. *ACS Sens.* **2021**, *6*, 130−136.
(13) Li, M.; Wang, L.; Liu, R.; Li, J.; Zhang, Q.; Shi, G.; Li, Y.; Hou, C.; Wang, H. A Highly Integrated Sensing Paper for Wearable Electrochemical Sweat Analysis. *Biosens. Bioelectron.* **2021**, *174*, 112828.
(14) Vaquer, A.; Barón, E.; de la Rica, R. Detection of Low Glucose Levels in Sweat with Colorimetric Wearable Biosensors. *Analyst* **2021**, *146*, 3273−3279.
(15) Yang, J.; Kwak, T. J.; Zhang, X.; McClain, R.; Chang, W.-J.; Gunasekaran, S. Digital PH Test Strips for In-Field PH Monitoring Using Iridium Oxide-Reduced Graphene Oxide Hybrid Thin Films. *ACS Sens.* **2016**, *1*, 1235−1243.
(16) Cunningham, J. C.; Kogan, M. R.; Tsai, Y.-J.; Luo, L.; Richards, I.; Crooks, R. M. Paper-Based Sensor for Electrochemical Detection of Silver Nanoparticle Labels by Galvanic Exchange. *ACS Sens.* **2016**, *1*, 40−47.
(17) Kim, S. B.; Zhang, Y.; Won, S. M.; Bandodkar, A. J.; Sekine, Y.; Xue, Y.; Koo, J.; Harshman, S. W.; Martin, J. A.; Park, J. M.; Ray, T. R.; Crawford, K. E.; Lee, K. T.; Choi, J.; Pitsch, R. L.; Grigsby, C. C.; Strang, A. J.; Chen, Y. Y.; Xu, S.; Kim, J.; Koh, A.; Ha, J. S.; Huang, Y.; Kim, S. W.; Rogers, J. A. Super-Absorbent Polymer Valves and Colorimetric Chemistries for Time-Sequenced Discrete Sampling and Chloride Analysis of Sweat via Skin-Mounted Soft Microfluidics. *Small* **2018**, *14*, 1−11.
(18) Choi, J.; Kang, D.; Han, S.; Kim, S. B.; Rogers, J. A. Thin, Soft, Skin-Mounted Microfluidic Networks with Capillary Bursting Valves for Chrono-Sampling of Sweat. *Adv. Healthcare Mater.* **2017**, *6*, 1−10.
(19) Rosenfeld, T.; Bercovici, M. Dynamic Control of Capillary Flow in Porous Media by Electroosmotic Pumping. *Lab Chip* **2019**, *19*, 328−334.
(20) Guo, Z. H.; Jiao, Y. C.; Wang, H. L.; Zhang, C.; Liang, F.; Liu, J. L.; Yu, H. D.; Li, C. M.; Zhu, G.; Wang, Z. L. Self-Powered Electrowetting Valve for Instantaneous and Simultaneous Actuation of Paper-Based Microfluidic Assays. *Adv. Funct. Mater.* **2019**, *29*, 1808974.
(21) Li, X.; Zwanenburg, P.; Liu, X. Magnetic Timing Valves for Fluid Control in Paper-Based Microfluidics. *Lab Chip* **2013**, *13*, 2609−2614.
(22) Jia, Y.; Sun, H.; Dong, H.; Wang, C.; Lin, X.; Dong, D. Scalable and Parallelized Biochemical Assays in Paper Devices Integrated with a Programmable Binary Valve Matrix. *Sens. Actuators, B* **2020**, *321*, 128466.
(23) Fu, H.; Song, P.; Wu, Q.; Zhao, C.; Pan, P.; Li, X.; Li-Jessen, N. Y. K.; Liu, X. A Paper-Based Microfluidic Platform with Shape-Memory-Polymer-Actuated Fluid Valves for Automated Multi-Step Immunoassays. *Microsyst. Nanoeng.* **2019**, *5*, 50.
(24) Zhang, J.; Huang, L.; Fan, Y.; Zhang, L.; Miao, G.; Xu, C.; Dong, X.; Liu, L.; Qiu, X. Programmable Thermally Actuated Wax Valve for Low-Cost Nonwoven-Based Microfluidic Systems. *Microsyst. Technol.* **2020**, *26*, 3847−3853.
(25) Chen, C.; Zhao, L.; Zhang, H.; Shen, X.; Zhu, Y.; Chen, H. Novel Wax Valves to Improve Distance-Based Analyte Detection in Paper Microfluidics. *Anal. Chem.* **2019**, *91*, 5169−5175.
(26) Lai, Y.-T.; Tsai, C.-H.; Hsu, J.-C.; Lu, Y.-W. Microfluidic Time-Delay Valve Mechanism on Paper-Based Devices for Automated Competitive ELISA. *Micromachines* **2019**, *10*, 837.
(27) Tu, D.; Holderby, A.; Dean, J.; Mabbott, S.; Coté, G. L. Paper Microfluidic Device with a Horizontal Motion Valve and a Localized Delay for Automatic Control of a Multistep Assay. *Anal. Chem.* **2021**, *93*, 4497−4505.
(28) He, X.; Liu, Z.; Yang, Y.; Li, L.; Wang, L.; Li, A.; Qu, Z.; Xu, F. Sensitivity Enhancement of Nucleic Acid Lateral Flow Assays through a Physical−Chemical Coupling Method: Dissoluble Saline Barriers. *ACS Sens.* **2019**, *4*, 1691−1700.
(29) Han, G. R.; Koo, H. J.; Ki, H.; Kim, M. G. Paper/Soluble Polymer Hybrid-Based Lateral Flow Biosensing Platform for High-Performance Point-of-Care Testing. *ACS Appl. Mater. Interfaces* **2020**, *12*, 34564−34575.
(30) Jahanshahi-Anbuhi, S.; Henry, A.; Leung, V.; Sicard, C.; Pennings, K.; Pelton, R.; Brennan, J. D.; Filipe, C. D. M. Paper-Based Microfluidics with an Erodible Polymeric Bridge Giving Controlled Release and Timed Flow Shutoff. *Lab Chip* **2014**, *14*, 229−236.
(31) Callewaert, C.; Buysschaert, B.; Vossen, E.; Fievez, V.; Van de Wiele, T.; Boon, N. Artificial Sweat Composition to Grow and Sustain a Mixed Human Axillary Microbiome. *J. Microbiol. Methods* **2014**, *103*, 6−8.
(32) Wiorek, A.; Parrilla, M.; Cuartero, M.; Crespo, G. A. Epidermal Patch with Glucose Biosensor: PH and Temperature Correction toward More Accurate Sweat Analysis during Sport Practice. *Anal. Chem.* **2020**, *92*, 10153−10161.
(33) Santopolo, G.; Doménech-Sánchez, A.; Russell, S. M.; De La Rica, R. Ultrafast and Ultrasensitive Naked-Eye Detection of Urease-Positive Bacteria with Plasmonic Nanosensors. *ACS Sens.* **2019**, *4*, 961−967.

https://doi.org/10.1021/acssensors.1c02244
ACS Sens. 2022, 7, 488−494